PCCP

Cite this: *Phys. Chem. Chem. Phys.*, 2011, **13**, 2797–2808

www.rsc.org/pccp

**PAPER**

# Charging of ionic liquid surfaces under X-ray irradiation: the measurement of absolute binding energies by XPS†

**Ignacio J. Villar-Garcia, Emily F. Smith, Alasdair W. Taylor, Fulian Qiu, Kevin R. J. Lovelock, Robert G. Jones and Peter Licence***

***Received 24th August 2010, Accepted 17th November 2010***
**DOI: 10.1039/c0cp01587c**

Ionic liquid surfaces can become electrically charged during X-ray photoelectron spectroscopy experiments, due to the flux of photoelectrons leaving the surface. This causes a shift in the measured binding energies of X-ray photoelectron peaks that depends on the magnitude of the surface charging. Consequently, a charge correction method is required for ionic liquids. Here we demonstrate the nature and extent of surface charging in ionic liquids and model it using chronopotentiometry. We report the X-ray photoelectron spectra for a range of imidazolium based ionic liquids and investigate the use of long alkyl chains ($C_nH_{2n+1}$, $n \geq 8$) and the imidazolium nitrogen, both of which are part of the ionic liquid chemical structure, as internal references for charge correction. Accurate and reproducible binding energies are obtained which allow comparisons to be made across ionic liquid-based systems.



## Introduction

Binding energies from X-ray photoelectron spectroscopy (XPS)[1] provide both elemental and chemical information and hence may be regarded as the most important pieces of data made available by the technique. The measurement of binding energies for a broad range of solid materials has been the subject of intense activity since the origins of XPS.[2–5] More recently XPS has been used to characterise ionic liquid-based samples,[6] to determine their purity,[7–13] and to probe both the chemical and physical behaviour occurring in ionic liquids and of solutes dissolved within them.[7,9–11,14–16] Binding energies have so far been used to characterise non-functionalised[7,14,15,17–20] and functionalised (“task-specific”) ionic liquids,[10,11,16,20–22] ionic liquid solutions[23–27] and the products of *in situ* ultra high vacuum electrochemical experiments.[28,29] If conclusions are to be drawn regarding subtle changes in chemistry within an ionic liquid, or a solute within the ionic liquid (*e.g.* it’s coordination environment),[6] then reliable binding energy data are required, such that confidence can be placed in the binding energy.[30]

In XPS, a sample is irradiated by X-rays, causing an electron flux consisting of photoelectrons, Auger electrons and secondary electrons to be emitted from the surface. The irradiated surface is left positively charged, generating a potential difference between the sample surface and its connection with earth (*i.e.* the metallic sample holder). For electrically conducting samples such as metals, their conductivity is sufficiently high (or their resistance is sufficiently low) that the flow of charge from earth is such that the potential difference between the earthed sample holder and the sample surface is orders of magnitude smaller than any measurable chemical shift. Hence, the surface of the sample may be considered to be at earth potential, and other earthed metals such as gold or silver can be used as calibrants for binding energy. However, for semi- or non-conducting samples, their increased resistance leads to a sizable (positive) potential difference between the irradiated surface and earth, causing the entire XP spectrum to shift to lower kinetic energies (*i.e.* higher apparent binding energies).[31,32] If the potential difference is substantial, the spectrum will also become distorted due to electric fields between the irradiated surface and the analyser (and other parts of the sample if a focussed X-ray beam is used). This process is called surface charging and in the case of good electrical insulators, the surface potential (in volts) could rise to the energy of the incident X-rays (in eV), thus preventing any electrons from leaving the surface. To make binding energy comparisons possible between experiments, charge control and charge correction methods must be applied.

Charge control methods aim to minimise the amount of charge (and hence positive potential) developing at the irradiated surface during an XPS experiment, while charge correction methods aim to correct for the potential post data collection. Charge neutralisation, the most common method of charge control, works by bathing the surface with a supply of low energy electrons (a few eV) in order to neutralise the

*School of Chemistry, The University of Nottingham, Nottingham NG7 2RD, UK. E-mail: peter.licence@nottingham.ac.uk; Tel: +44 (0)115 8466176*

† Electronic supplementary information (ESI) available: XP spectra and peak fitting models for all $[C_8C_1Im][X]$-based ionic liquids studied. See DOI: 10.1039/c0cp01587c

positive charge developed during the XPS experiment. Charge neutralisation, using a simple hot filament, overcomes any positive charging of the surface of an insulating material, but overcompensation can occur leading to the sample becoming slightly negatively charged.[31,33] Accordingly, post experiment charge correction methods should be applied to get an accurate binding energy scale.

Most charge correction methods (or *calibration of the energy scale*[34]) involve referencing to a "standard" peak of known binding energy within the collected spectrum. Internal referencing, where the standard is commonly part of the surface being analysed, is considered the most accurate method, as any surface charging effects will be experienced equally by both the reference and the sample.[31,33,35] If the true binding energy of the reference material is known, then the true, or absolute, binding energies of all other components within the spectrum are calibrated. However, as the "standard" binding energies employed in energy scale calibration can vary, *e.g.* the most commonly used internal standard is aliphatic carbon, where the binding energy value for C 1s can be set to either 284.8 or 285.0 eV, the value employed should be noted.

High quality XP spectra of ionic liquids have been obtained with good signal-to-noise ratios and narrow full width half maxima (FWHM) without the use of charge control methods.[10,11,13,15–20,36] The ability to collect XPS data of this quality without charge neutralisation is characteristic of electrically conducting samples. However, problems with obtaining reproducible binding energies for a number of different ionic liquids have been reported.[9,11,13,19] As ionic liquids are ionic conductors and not electron conductors, they become insulators when frozen to the solid state (either crystalline or glassy) and hence require charge neutralisation to avoid surface charging in XPS.[12,19,36] A number of groups have concluded that using an internal reference is necessary to obtain true binding energies of ionic liquid samples, even if they are in their liquid state. It is becoming common practice to charge correct by referencing spectra to the signal of the aliphatic carbon atoms ($C_{aliphatic}$ 1s) present in most ionic liquids (binding energy = 285.0 eV in most cases).[15,18,25,27,37–44] The causes of these binding energy acquisition problems have not been ascertained and often XPS data obtained from ionic liquids are not charge corrected.[14,17,23,24,26,45,46] Here we demonstrate the nature and extent of surface charging in ionic liquids, model it using chronopotentiometry, and propose a robust method of charge correction using the alkyl chains and the imidazolium nitrogens within the ionic liquid itself.

## Experimental

### Materials

All ionic liquids investigated in this study were prepared in our laboratory using established synthetic methods: $[C_2C_1Im]Cl$,[47] $[C_nC_1Im]Cl$ ($n$ = 4, 8, 12),[48] $[C_nC_1Im]Br$ ($n$ = 2, 4, 8, 12),[49,50] $[C_nC_1Im][PF_6]$ ($n$ = 2, 4, 8, 12),[48] $[C_nC_1Im][BF_4]$ ($n$ = 2, 4, 8, 12),[51] $[C_nC_1Im][Tf_2N]$ ($n$ = 2, 4, 8, 12),[49,50] $[C_nC_1Im][TfO]$ ($n$ = 1, 2, 4, 8, 12),[52] $[C_nC_1Im][N(CN)_2]$ ($n$ = 2, 4, 8, 12),[53] $[C_2C_1Im][EtOSO_3]$.[54] The purity of all ionic liquid samples was assessed using $^1H$ NMR and $^{13}C$ NMR spectroscopy. When anion exchange was one of the synthetic steps, ion chromatography analysis showed that halide contamination was below 10 ppm for $[PF_6]^-$ and $[Tf_2N]^-$ based ionic liquids and below 1000 ppm for $[BF_4]^-$, $[TfO]^-$ and $[N(CN)_2]^-$ based ionic liquids. No halide signal was observed by XPS analysis, *i.e.* the concentration was below the limit of detection in every case. The structures of the individual ions investigated in this study are shown in Table 1.

**Table 1** Structure of the polyatomic ionic components investigated in this study. Ionic liquids based upon simple halides, $Cl^-$, $Br^-$, and $I^-$, were also investigated

| Abbreviation | Structure | Name |
|---|---|---|
| $[C_nC_1Im]^+$ | 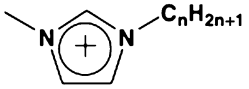 | 1-Alkyl-3-methylimidazolium |
| $[BF_4]^-$ | 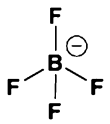 | Tetrafluoroborate |
| $[EtOSO_3]^-$ | 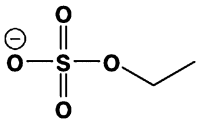 | Ethylsulfate |
| $[Tf_2N]^-$ | 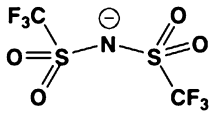 | Bis[(trifluoromethane)-sulfonyl]imide |
| $[TfO]^-$ | 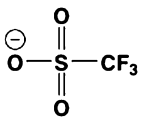 | Trifluoromethanesulfonate |
| $[PF_6]^-$ | 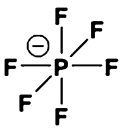 | Hexafluorophosphate |
| $[N(CN)_2]^-$ | 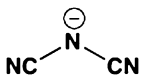 | Dicyanamide |

### XPS data collection

All XP spectra were recorded using a Kratos Axis Ultra spectrometer employing a focused, monochromated Al Kα source ($h\nu$ = 1486.6 eV), hybrid (magnetic/electrostatic) optics, hemispherical analyser and a multi-channel plate and delay line detector (DLD) with a X-ray incident angle of 30° and a collection angle of 0° (both relative to the surface normal). X-ray gun power was set to 150 W. All spectra were

 

recorded using an entrance aperture of 300 × 700 μm with a pass energy of 80 eV for wide scans and 20 eV for high-resolution scans. The instrument sensitivity was $7.5 \times 10^5$ counts $s^{-1}$ when measuring the Ag $3d_{5/2}$ photoemission peak for a clean Ag sample recorded at a pass energy of 20 eV and 450 W emission power. Ag $3d_{5/2}$ FWHM was 0.55 eV for the same instrument settings. Binding energy calibration was made using Au $4f_{7/2}$ (83.96 eV), Ag $3d_{5/2}$ (368.21 eV) and Cu $2p_{3/2}$ (932.62 eV). The absolute error in the acquisition of binding energies is ±0.1 eV, as quoted by the instruments manufacturer (Kratos). Charge neutralisation, when used, was applied using a standard Kratos charge neutraliser consisting of a filament, coaxial with the electrostatic and magnetic transfer lenses, and a balance plate which creates a potential gradient between the neutraliser and sample. Charge neutralisation was applied at 1.9 A filament current and 3.3 V balance plate voltage. Sample stubs were earthed *via* the instrument stage to the UHV chamber.

Samples were prepared by placing a small drop (< 10 mg) of the ionic liquid into a depression on a stainless steel sample stub (designed for powders) or on a standard stainless steel multi-sample bar (both Kratos designs). Samples were introduced into the instrument immediately after preparation to avoid absorption of moisture. Initial pumping was carried out in a preparation chamber, until the pressure was $\sim 10^{-7}$ mbar, and the sample was then transferred to the main analytical vacuum chamber. In general, pumping times were rapid, achieving the required vacuum in the main chamber ($< 1 \times 10^{-8}$ mbar) after approximately 60 min. However, pumping-times varied depending upon the volume, volatile impurity content and viscosity of the sample, *i.e.*, viscous ionic liquids were found to require longer pumping times. For clarity, a full description of the data analysis is included below; full experimental details and discussion of the fitting procedures are published elsewhere.[6,13,19,55]

## XPS data analysis

For data interpretation, two point linear and Shirley background subtractions were used depending upon the shape of the spectrum. Relative Sensitivity Factors (RSF) were taken from the Kratos Library (RSF of F 1s = 1) and were used to determine atomic percentages.[56] Peaks were fitted using GL(30) lineshapes, a combination of Gaussian (70%) and Lorentzian (30%).[1] This lineshape has been used consistently in the fitting of XP spectra, and has been found to match experimental lineshapes in ionic liquid systems.[19] The FWHM of each component was initially constrained to $0.8 \leq \text{FWHM} \leq 1.5$ eV.

## Fitting procedure for 1-alkyl-3-methylimidazolium-based $[C_nC_1Im][X]$ ionic liquids

The high resolution C 1s scans of imidazolium-based ionic liquids were fitted based upon an established model employed in previous studies.[13,19,37] Here we describe a representative example of this analysis, using $[C_8C_1Im][TfO]$, see Fig. 1. The high resolution C 1s photoelectron spectrum of non-functionalised imidazolium-based ionic liquids is composed of two partially resolved peaks (~285.0 eV and 286.8 eV), the peak at higher binding energy having a characteristic shoulder (~287.5 eV). In Fig. 1 there is also a peak (292.5 eV) due to the $CF_3$ in the $[TfO]^-$ anion.

Five components were used to fit the C 1s experimental spectrum for $[C_8C_1Im][TfO]$, based upon the distinct chemical environments identified in Fig. 1.[13,19,37] Structurally diverse ionic liquids may require more or less components, dependent upon the number of distinct chemical environments present. Based upon established literature values, the peak at 285.0 eV is fitted with one component ($C_{aliphatic}$), the peak at 286.0–288.0 eV with three components corresponding to $C^2$, ($C^4 + C^5$), ($C^6 + C^7$) and the peak at 292.5 eV with a single component ($CF_3$). From a closer analysis of their chemical environments, $C^2$ is expected to exhibit the highest binding energy as it is bonded to two (relatively more electronegative) nitrogen atoms. Consequently, it sits beneath the shoulder of the partially resolved peak at the higher binding energy. ($C^4 + C^5$) and ($C^6 + C^7$) are differentiated in our model based upon the observation that ($C^4 + C^5$) is part of the positively charged imidazolium ring and is expected to have a higher binding energy than the saturated ($C^6 + C^7$) atoms.

As there are a total of 13 C atoms in $[C_8C_1Im][TfO]$, it would be expected that the stoichiometric ratio of

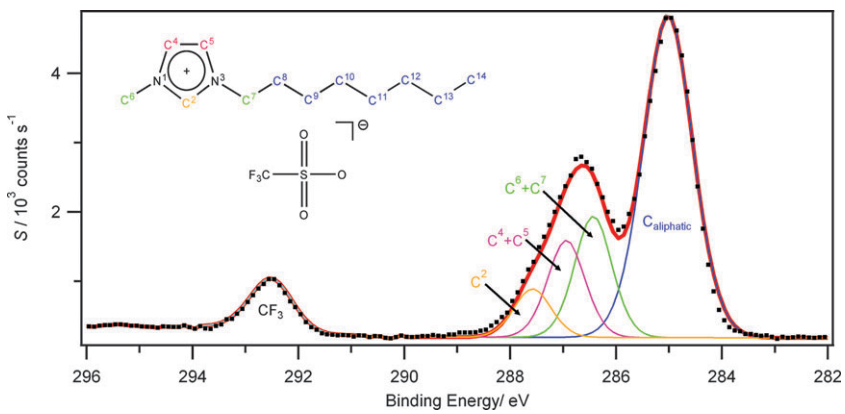


**Fig. 1** $[C_8C_1Im][TfO]$ C 1s high resolution scan and fitting. The spectrum has been fitted using five components, $CF_3$, $C^2$, ($C^4 + C^5$), ($C^6 + C^7$) and ($C^8 + C^9 + \ldots C^{14}$) = $C_{aliphatic}$. The inset structure shows the numbering system used in the deconstruction and fitting of the C 1s photoemission envelope of imidazolium-based ionic liquids. Note, carbons numbered >8 are collectively known as $C_{aliphatic}$.

these different components should equate to 1 : 1 : 2 : 2 : 7 ($CF_3$ : $C^2$ : ($C^4$ + $C^5$) : ($C^6$ + $C^7$) : $C_{aliphatic}$). However, shake up satellites can be observed as broad features in the spectrum at 291.5–295.5 eV. Such features can be noted at similar binding energies to the $-CF_3$ feature (292.5 eV) in Fig. 1. Approximately 20% of all photoelectrons originating from the imidazolium ring will be affected by shake up/off phenomena and the corresponding C 1s peaks should be fitted to account for this redistribution, *i.e.* by reducing the total component areas for $C^2$ and ($C^4$ + $C^5$) by 20%.[19,55] As the peak areas for the signals characteristic of aliphatic carbons are not affected by the shake up/off phenomenon, the relative peak area ratios for the four cationic components can now be set to 0.8 : 1.6 : 2 : 7 for $C^2$ : ($C^4$ + $C^5$) : ($C^6$ + $C^7$) : $C_{aliphatic}$. The FWHM values are set to be equal for the $C^2$, ($C^4$ + $C^5$) and ($C^6$ + $C^7$) components (and constrained to be close to unity: 0.8 ≤ FWHM ≤ 1.2), *e.g.* for $[C_8C_1Im][TfO]$ the FWHM for these components is 0.93 eV.[32,57] The FWHM for $C_{aliphatic}$ 1s is separately constrained as it has been shown to produce a broader signal, *e.g.* for $[C_8C_1Im][TfO]$ the FWHM is 1.09 eV.[58,59] In general for all ionic liquids studied here, measured FWHM values for $C_{aliphatic}$ 1s are typically ~0.2 eV larger than for the other imidazolium-based carbon atoms. The fit shows an excellent agreement to the experimentally acquired signal for $[C_8C_1Im][TfO]$, see Fig. 1. This procedure was used to fit the measured XP spectra of all $[C_8C_1Im][X]$ ionic liquids studied during this work.

### Chronopotentiometry

All chronopotentiometry experiments were performed using an Autolab 30 potentiostat. A Mo XPS sample stub was loaded with $[C_2C_1Im][Tf_2N]$ and a Pt working electrode (area = 0.196 $mm^2$) was placed in contact with the ionic liquid, see Fig. 4b. The sample stub acted as the counter electrode completing a simple two electrode cell. The working electrode area was within an order of magnitude of that of the area illuminated by X-rays in a typical XPS experiment (approximately 1 $mm^2$). The thickness of the ionic liquid employed during chronopotentiometry was greater than that employed in a typical XPS analysis (approximately 2 mm) to avoid electrical shorting of the Pt electrode (working) with the stub (counter).

## Results and discussion

### Charging of ionic liquids under the X-ray beam—defining the problem

Fig. 2 illustrates XP spectra acquired during three different sets of experimental scans recorded on separate days using different aliquots of the same sample, $[C_4C_1Im][PF_6]$. No charge control or charge correction methods were applied to the measurement of these scans. These spectra highlight reproducibility problems that may be encountered when analysing ionic liquids by XPS. The binding energies for all elements analysed were observed to shift by as much as 0.8 eV between the different analyses, but all the elements in a particular analysis on a particular day were shifted by the same amount (within experimental error). The intensity differences are due to a number of additive experimental parameters, including sample height, geometry and system pressure. An uncertainty of 0.8 eV is unacceptable for XPS analysis, as differences between the different chemical states of an element can cause much more subtle shifts in binding energy. For example, the XPS peaks arising

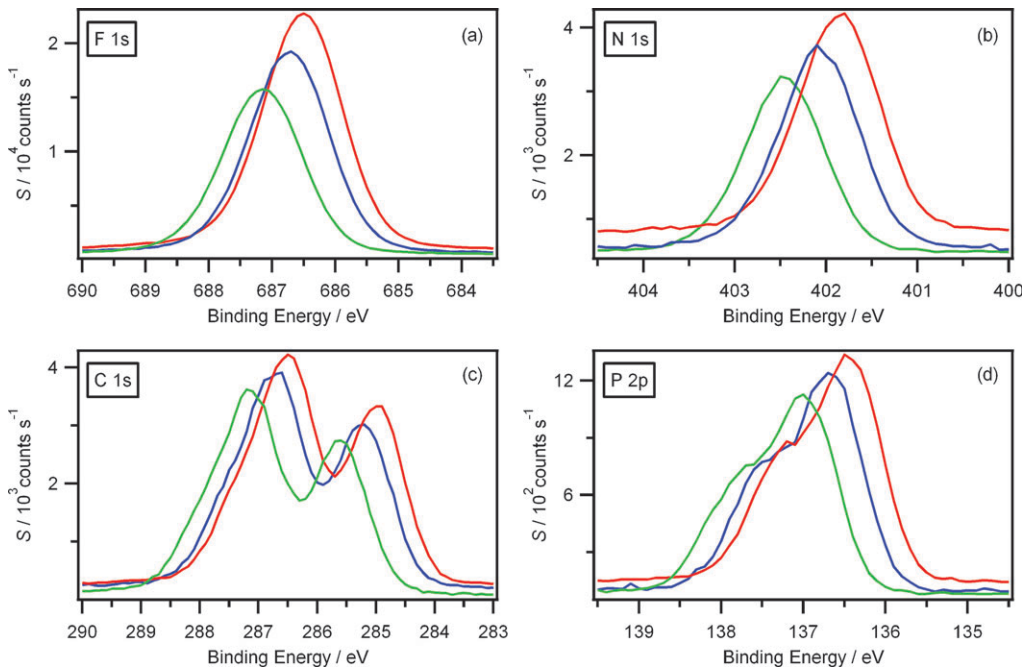


**Fig. 2** (a) F 1s, (b) N 1s, (c) C 1s and (d) P 2p high resolution XP spectra of $[C_4C_1Im][PF_6]$ acquired from different aliquots of the same sample recorded on three separate occasions. All element signals experienced a similar change, both in signal magnitude (*S*) and absolute value of the binding energy. No charge control or charge correction methods were applied during these experiments.

 

from different oxidation states of a metal may be separated by less than 0.8 eV.[30] Therefore, understanding the causes of these reproducibility problems is critical to ensure the acquisition of accurate binding energy data, especially in systems where very subtle changes in binding energy are expected.

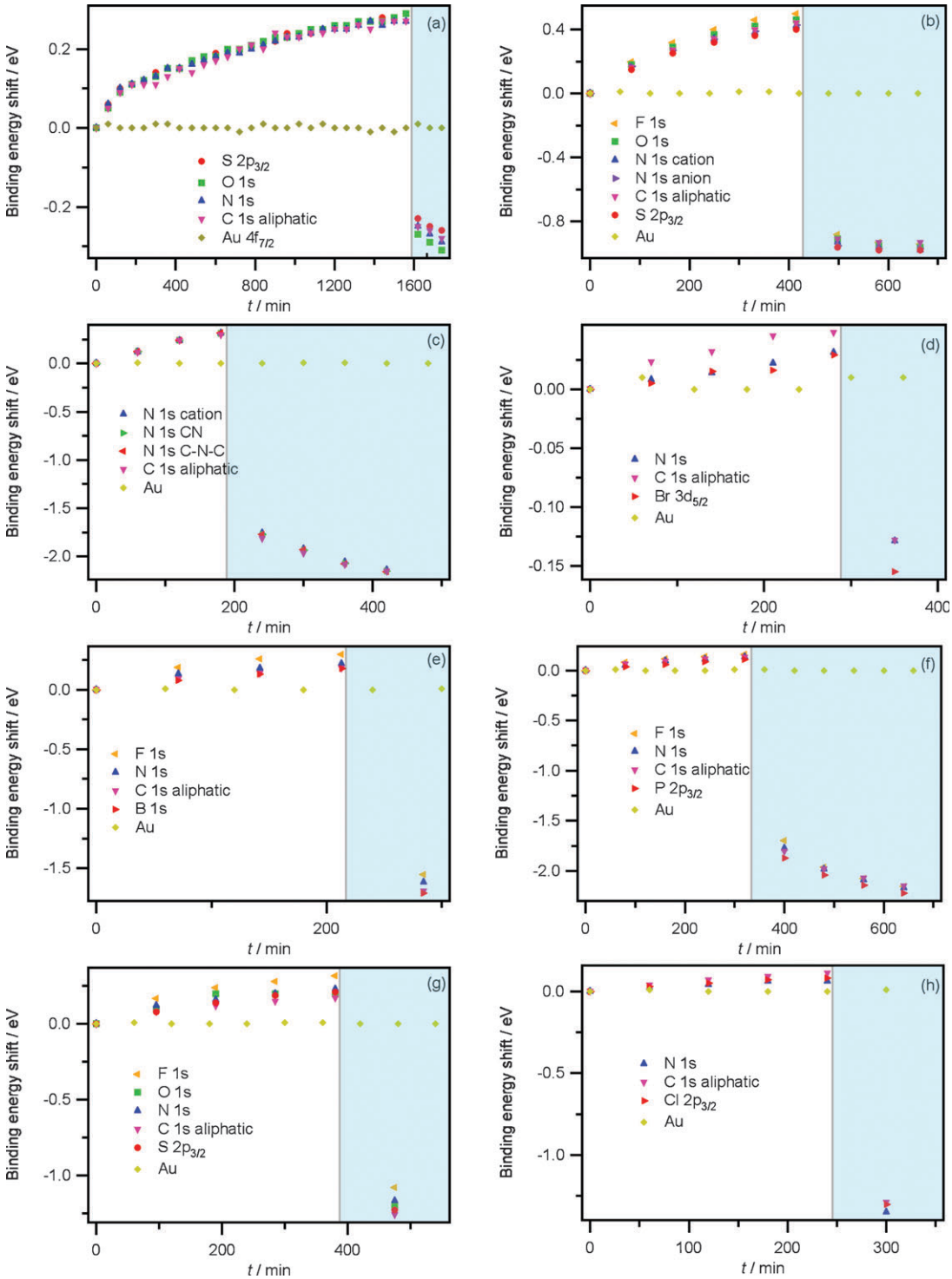


**Fig. 3** Typical example of the variation of the binding energies measured when analysing an ionic liquid by XPS as a function of time, both with and without charge neutralisation. (a) $[C_2C_1Im][EtOSO_3]$, (b) $[C_8C_1Im][Tf_2N]$, (c) $[C_8C_1Im][N(CN)_2]$, (d) $[C_8C_1Im]Br$, (e) $[C_8C_1Im][BF_4]$, (f) $[C_8C_1Im][PF_6]$, (g) $[C_8C_1Im][TfO]$ and (h) $[C_8C_1Im]Cl$. Binding energy shifts, relative to the first scan acquired when $t = 0$ min, are monitored for each component in the ionic liquid sample and a gold slide substrate (Au $4f_{7/2}$). Note the use of charge neutralisation is clearly identified (shaded area of plots). The measured binding energy of all components is observed to take a significant step (−ve) when charge neutralisation is employed.

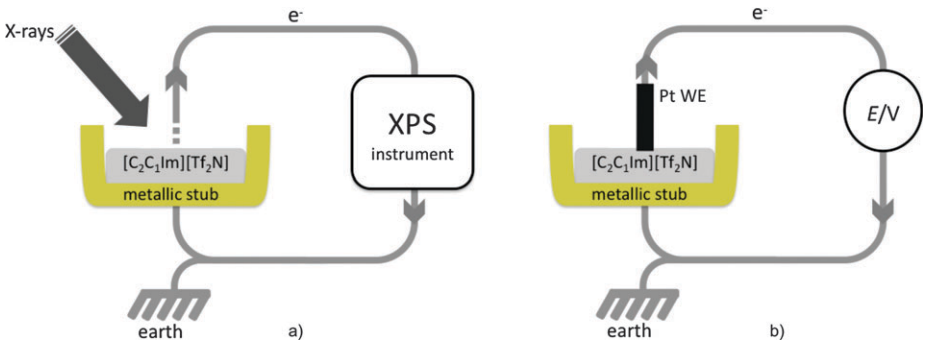


**Fig. 4** (a) Schematic representation of a typical XPS experiment on $[C_2C_1Im][Tf_2N]$ as an electrical circuit; (b) schematic of the model chronopotentiometry experimental set up, employing a Pt working electrode (Pt WE), used to mimic the photoelectric process occurring inside the XP spectrometer.

To investigate these shifts, a range of ionic liquids were exposed to the X-ray beam for up to 1800 min and high resolution scans for each element were taken periodically (every 10 min). Charge neutralisation was then applied to each sample after a prolonged exposure to the X-ray beam. Fig. 3 shows the characteristic binding energies for each element in a range of ionic liquids over the course of the experiment, as well as binding energies of the Au 4f peaks recorded during a separate control experiment using a gold slide substrate, *i.e.*, an electrically conducting metallic sample. Here we describe the results for $[C_2C_1Im][EtOSO_3]$, Fig. 3a, as an example of the general trend followed by all the ionic liquids analysed, Fig. 3b–h. The measured Au 4f binding energy does not shift during the first 1600 min of exposure to the X-ray beam and does not shift when charge neutralisation is applied to the surface; this behaviour is exactly what one would expect for a good metallic conductor such as gold. On the other hand, for $[C_2C_1Im][EtOSO_3]$, Fig. 3a, during the first 1600 min of X-ray irradiation without charge neutralisation there is a clear shift in all the binding energies to higher values, reaching a shift of $+0.3$ eV after 1440 min. This shift is consistent with the ionic liquid surface becoming positively charged. When charge neutralisation was switched on (at $t > 1600$ min in Fig. 3a), the ionic liquid peaks all moved abruptly to a negative binding energy shift, consistent with the surface now charging negatively from the incident electrons used for charge neutralisation. Further exposure to charge neutralisation (*i.e.* impinging electrons) caused the binding energy shift to increase in the negative sense (*i.e.* increasingly negative surface charge). The gradual changes in binding energy shifts under both X-ray irradiation and impinging electrons from the charge neutraliser point towards a sluggish conduction mechanism within the ionic liquid that is tending towards an equilibrium surface charge. Similar results can be seen for the other ionic liquids, Fig. 3b–h.

At this point, we note that no chemical changes were observed during the analysis of any of the ionic liquids, *i.e.* all peaks remained fixed in binding energy and intensity relative to the other peaks taken at the same time, within experimental error. Also, on switching off the X-ray source (and charge neutraliser), and leaving the sample in the vacuum chamber overnight, the photoelectron peaks of the ionic liquids were found to have returned to binding energies similar to those recorded at the start of the previous day. In summary, the surface charging appears to be reversible.

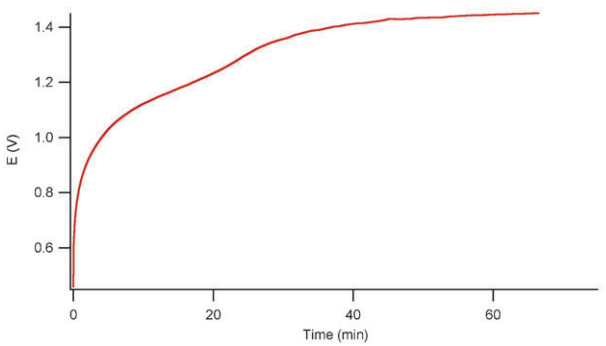


**Fig. 5** Potential ($E$) developed as a function of time during the course of a chronopotentiometry experiment using the experimental set-up shown in Fig. 4b on a sample of $[C_2C_1Im][Tf_2N]$.

### Chronopotentiometric simulation of a charged surface

The results shown in Fig. 3 indicate that the conductivities of ionic liquids are not sufficient to neutralise the surface charge

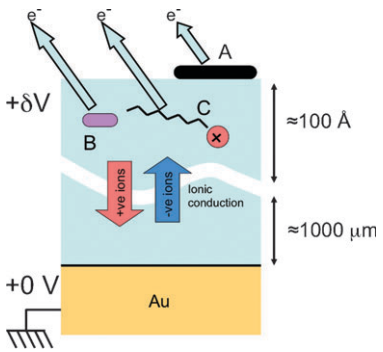


**Fig. 6** Internal calibrants that may be used to charge correct ionic liquid-based samples. A key point is that the calibrant must be at the same potential as the photoemitting surface of the ionic liquid (top 100 Å): (A) adventitious carbon on the sample surface; (B) adventitious carbon (or an alternative calibrant material) dissolved in the sample; (C) a constituent part of the sample itself, such as the alkyl chain or the imidazolium nitrogen.

 

created during XPS experiments recorded on a time scale of minutes to hours. The XPS experiment can be considered as equivalent to an electric circuit, Fig. 4a. This circuit was then modelled by designing a chronopotentiometric experiment using a two-electrode electrochemical cell, Fig. 4b.

The total photocurrent from a sample of ionic liquid was a few nA (X-ray gun power = 150 W). Therefore, a positive current of 10 nA was used in the chronopotentiometric experiments and the potential difference generated between the working electrode and stub (counter electrode) was monitored as a function of time, Fig. 5. Upon applying the current, the potential difference across the ionic liquid rose rapidly within the first 5 min of the experiment. Over the course of the next hour, it then rose more slowly until reaching an equilibrium value of $\sim +1.4$ V. Whilst there are clear differences between the way electrons are removed from the ionic liquid in the XPS and chronopotentiometric experiments, a similar, slow rise in potential difference across the ionic liquid is common to both (within an order of magnitude). As binding energies are measured relative to the potential of the spectrometer (and not the surface of the sample), this potential difference will affect the binding energies obtained, thereby explaining the shifts observed when analysing ionic liquids by XPS over time. These results support the idea that the variation of surface charging during an XPS experiment, leading to the creation of a potential difference between the liquid surface and the spectrometer, is a consequence of conduction through the ionic liquid.

Ionic conduction, as found in ionic liquids, involves movement of ions and is inherently different to electronic conduction in metals and semiconductors, which involves the movement of electrons within the band structure. Within the bulk of the ionic liquid, between the earthed substrate and the ionic liquid surface, the anions and cations that constitute the ionic liquid move under the action of the electric field caused by surface charging, see Fig. 6. The study of this mechanism is the subject of ongoing research in our group but the important parameters can be summarised as follows. The total photocurrent from the surface, $I$, has to be carried by ionic conduction through the ionic liquid, from the metallic substrate to the ionic liquid surface. This ionic conduction has a resistance $R$, where $R$ depends on the magnitude of the current itself (and hence on X-ray wavelength, flux, angle of incidence, and photoionisation cross sections of the atoms in the sample material as well as the nature of the surface and as exhibited by its Auger and secondary electron emission characteristics) and on the conduction mechanism of the ions (which depends on the nature of the ions, their transport properties, and the path length from earthed substrate to ionic liquid surface). The potential difference, $V$ ($= IR$), between the substrate (at earth) and the X-ray irradiated surface of the ionic liquid (at a positive $V$), is therefore a function of the incident X-rays, the sample geometry and the nature of the ionic liquid. We have shown above that for the ionic liquids in this study, the conduction mechanism is insufficient to avoid the slow attainment of a surface charge that is large enough to affect the accurate measurement of chemical shifts in XPS. At present we are investigating the correlation between ionic liquid viscosity and conductivity and the magnitude of $V$.

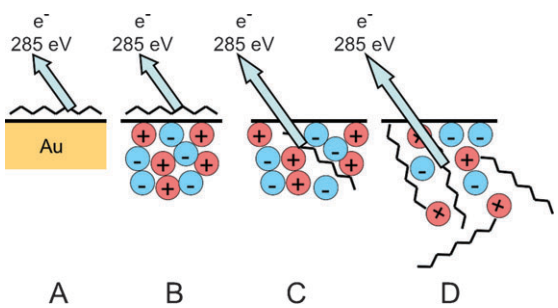


**Fig. 7** Diagram to illustrate: (A) adventitious carbon on gold; (B) adventitious carbon on an ionic liquid; (C) adventitious carbon or hydrocarbon dissolved in an ionic liquid; (D) alkyl chain covalently bonded to the cationic moiety.

### Charge correction of ionic liquids using internal referencing

Historically, charge correction of solid salts has been made by calibration to the $C_{aliphatic}$ 1s component of (adventitious) carbon contamination on the sample surface,[60–63] the method being generally applicable to any XPS sample with such contamination, Fig. 6, method A.[31] Internal referencing, using a probe species doped into the sample, Fig. 6, method B, or using a species that is a constituent of the sample itself, Fig. 6, method C, offers a more reliable and accurate method. As for any correction for an effect which changes with time, it is necessary to ensure that the scan across the calibrant is sufficiently close in time, or better still that it brackets (before and after)[64] the spectrum being calibrated, to ensure its validity.

### Is the aliphatic chain used for internal referencing of ionic liquids truly aliphatic?

In the majority of XPS studies of ionic liquids, charge correction is achieved using the aliphatic carbon atoms of the cation alkyl chain, where the $C_{aliphatic}$ 1s peak is commonly corrected to 284.8 or 285.0 eV.[30,65] However, we must question if this assumption is appropriate for charge correction of all ionic liquid-based samples.

Fig. 7A shows adventitious aliphatic carbon on gold, which can be assigned a binding energy of 285.0 eV. In Fig. 7B the adventitious aliphatic carbon is at the surface of an ionic liquid. In reality, even without surface charging, such a surface species is probably at a different potential to the aliphatic carbon on gold. In Fig. 7C the adventitious alkyl chain is now dissolved in the ionic liquid and the carbon chain is probably at a different potential to those in both Fig. 7A and B. In Fig. 7D the alkyl chain is attached to the cation of the ionic liquid and this is the method most commonly used for calibration of XP spectra of $[C_nC_1Im][X]$ ionic liquids. However, it has been shown that for short chain $[C_nC_1Im][Tf_2N]$ ($n < 8$) ionic liquids, the binding energy of the $C_{aliphatic}$ 1s peak is dependent upon the length of the alkyl chain.[11] The possible contributing factors that cause this shift

in binding energy of the $C_{aliphatic}$ 1s when $n < 8$ are now described.

Ionic liquids can be thought of in terms of two continuous, interpenetrating but nearly independent domains, one of which is predominantly aliphatic and hydrophobic in nature and a second which is more polar and composed of the ionic parts of the ionic liquid.[66] As the alkyl chain length increases, the nanostructural organisation locates the alkyl carbons in a hydrocarbon rich environment, minimising any interactions with the polar, or charged head groups, giving rise to a situation chemically similar to simple hydrocarbon, see Fig. 7A. Thus we can assign a binding energy of 285.0 eV to the alkyl chains on the cations, arguing that the electrostatic potential of the alkyl chain on a gold surface (work function ≈ 5.4 eV) is likely to be similar to the effective work function of an alkyl chain embedded in the ionic liquid. In this way, charge correction of XP spectra of ionic liquids using the alkyl carbon should provide binding energies comparable to other literature values. However, as the aliphatic chains are attached to the cationic component of the ionic liquid we need to consider which part of the aliphatic chain to use. The aliphatic carbons closest to the imidazolium ring ($C^8$ to $C^{10}$ in Fig. 1) are influenced by the electron withdrawing effect of the ring, and their binding energies are expected to be slightly higher than 285.0 eV.[18] As the chain length increases, the higher numbered carbons are located further away from the influence of the imidazolium ring and their binding energies should sit at 285.0 eV. This behaviour explains the shift in binding energies observed previously for the $C_{aliphatic}$ 1s peak of a series of $[C_nC_1Im][Tf_2N]$ ionic liquids.[11] In this particular case, the binding energy was observed to shift −0.4 eV from $n = 2$ to $n = 8$ with no further shift observed for $n = 8$ to 16. Therefore, only when the alkyl chain is long ($n \geq 8$), do we expect the binding energies for the $C_{aliphatic}$ 1s to be a reliable reference.

### Can other atoms within the ionic liquid be used for internal reference?

The variance in binding energy of $C_{aliphatic}$ 1s when $n < 8$ poses a problem if we want a reliable internal reference for all $[C_nC_1Im][X]$-based ionic liquids. However, the binding energies of the atoms within the $[Tf_2N]^-$ anion, and those of the imidazolium ring itself, might not be expected to vary in binding energy with alkyl chain length. If this observation is true for all of the ionic liquids studied, then the binding energy of any element within the anion or the imidazolium ring could, in principle, be used as internal reference for all ionic liquids containing the same anion and similar cations. We now test these ideas.

### Testing the charge correction hypothesis

A wide range of ionic liquids of the type $[C_8C_1Im][X]$ (where X = Cl, Br, $PF_6$, $BF_4$, $Tf_2N$, TfO, $N(CN)_2$) were analysed by XPS and divided into families, where each family contained a common anion. By taking the $[C_8C_1Im][X]$ ionic liquids in each family, we could confidently charge correct the $C_{aliphatic}$ 1s peak to 285.0 eV and then obtain reliable binding energies for the $N_{cation}$ 1s, as well as all the other components in each ionic liquid (Table 2). The binding energies of the rest of the $[C_nC_1Im][X]$ ionic liquids in each family (where $n = 2$, 4, 12) were then charge corrected using the $N_{cation}$ 1s binding energy obtained for the $[C_8C_1Im][X]$ member, see Table 3.

If we consider the data presented in Table 3, it can be seen that, within each family of ionic liquids studied, the binding energies of the atoms within the anion and the imidazolium ring are relatively "stable" and do not shift significantly, regardless of the length of the alkyl chain. This observation suggests that the binding energies of any of these atoms may, in principle, be used to charge correct other ionic liquid-based samples from within that same family. This observation is shown more clearly in Fig. 8, which illustrates binding energies for each component within the ionic liquid relative to the values obtained for the $[C_8C_1Im][X]$ member.

In all these plots $N_{cation}$ 1s is a horizontal line at zero, as this was used to calibrate the spectra. The $C^2$, ($C^4$ + $C^5$) and ($C^6$ + $C^7$) components show no particular trend in behaviour for increasing chain length. For each family of ionic liquids, except when X = Cl, Br, the $C_{aliphatic}$ 1s binding energy decreases as the alkyl chain length increases from $n = 2$ to 8, after which no further change is observed.

**Table 2** Binding energies for a series of commonly used ionic liquids of the general formula $[C_8C_1Im][X]$. All binding energies are determined after charge correction of the measured XP spectra by setting $C_{aliphatic}$ 1s = 285.0 eV. (See ESI† for all XP spectra, survey and high-resolution scans, and peak fitting models used in collection of these data)

| | Cation | | | | | Anion | | | | | | | | | |
|---|---|---|---|---|---|---|---|---|---|---|---|---|---|---|---|
| Anion for $[C_8C_1Im][X]$ | C 1s Aliphatic | C 1s $C^6$ + $C^7$ | C 1s $C^4$ + $C^5$ | C 1s $C^2$ | N 1s | C 1s | N 1s | N 1s | O 1s | S $2p_{3/2}$ | B 1s | P $2p_{3/2}$ | F 1s | Cl $2p_{3/2}$ | Br $3d_{5/2}$ | I $3d_{5/2}$ |
| $Cl^-$ | 285.0 | 286.2 | 286.6 | 287.3 | 401.7 | | | | | | | | | 197.1 | | |
| $Br^-$ | 285.0 | 286.2 | 286.7 | 287.4 | 401.7 | | | | | | | | | | 67.5 | |
| $I^-$ | 285.0 | 286.3 | 286.8 | 287.4 | 401.9 | | | | | | | | | | | 618.5 |
| $[N(CN)_2]^-$ | 285.0 | 286.6 | 287.0 | 287.5 | 402.0 | 286.6 | 398.3[a] | 399.6[b] | | | | | | | | |
| $[BF_4]^-$ | 285.0 | 286.4 | 286.8 | 287.6 | 402.0 | | | | | | 194.3 | | 686.0 | | | |
| $[PF_6]^-$ | 285.0 | 286.5 | 287.0 | 287.7 | 402.1 | | | | | | | 136.6 | 686.7 | | | |
| $[TfO]^-$ | 285.0 | 286.4 | 286.9 | 287.6 | 402.0 | 292.5 | | | 532.0 | 168.5 | | | 688.4 | | | |
| $[Tf_2N]^-$ | 285.0 | 286.6 | 287.0 | 287.7 | 402.1 | 292.9 | | 399.5 | 532.7 | 169.0 | | | 688.8 | | | |

[a] $N(CN^*)_2$. [b] $N^*(CN)_2$.

 

**Table 3** Binding energies for a series of commonly used ionic liquids after charge correcting using the $N_{cation}$ 1s binding for the $[C_8C_1Im][X]$ member of each anion [X] family

| | | Cation | | | | | Anion | | | | | | | | | |
|---|---|---|---|---|---|---|---|---|---|---|---|---|---|---|---|---|
| Anion for $[C_nC_1Im][X]$ | $n$ for $[C_nC_1Im][X]$ | C 1s Aliphatic | C 1s $C^6 + C^7$ | C 1s $C^4 + C^5$ | C 1s $C^2$ | N 1s | C 1s | N 1s | N 1s | O 1s | S $2p_{3/2}$ | B 1s | P $2p_{3/2}$ | F 1s | Cl $2p_{3/2}$ | Br $3d_{5/2}$ |
| $Cl^-$ | 2 | 285.1 | 286.1 | 286.6 | 287.2 | 401.7 | | | | | | | | | 197.1 | |
| | 4 | 285.1 | 286.1 | 286.5 | 287.3 | 401.7 | | | | | | | | | 197.2 | |
| | 8 | 285.0 | 286.2 | 286.6 | 287.3 | 401.7 | | | | | | | | | 197.1 | |
| | 12 | 285.1 | 286.2 | 286.5 | 287.3 | 401.7 | | | | | | | | | 197.1 | |
| $Br^-$ | 2 | 285.1 | 286.3 | 286.6 | 287.3 | 401.7 | | | | | | | | | | 67.5 |
| | 4 | 285.1 | 286.2 | 286.6 | 287.3 | 401.7 | | | | | | | | | | 67.5 |
| | 8 | 285.0 | 286.2 | 286.7 | 287.4 | 401.7 | | | | | | | | | | 67.5 |
| | 12 | 285.0 | 286.3 | 286.6 | 287.3 | 401.7 | | | | | | | | | | 67.5 |
| $[N(CN)_2]^-$ | 2 | 285.4 | 286.6 | 286.9 | 287.6 | 402.0 | 286.9 | 398.4[a] | 399.7[b] | | | | | | | |
| | 4 | 285.2 | 286.7 | 286.7 | 287.5 | 402.0 | 286.7 | 398.3[a] | 399.6[b] | | | | | | | |
| | 8 | 285.0 | 286.6 | 287.0 | 287.5 | 402.0 | 286.6 | 398.3[a] | 399.6[b] | | | | | | | |
| | 12 | 285.0 | 286.6 | 287.0 | 287.5 | 402.0 | 286.6 | 398.3[a] | 399.6[b] | | | | | | | |
| $[BF_4]^-$ | 2 | 285.3 | 286.4 | 286.9 | 287.6 | 402.0 | | | | | | 194.2 | | 686.0 | | |
| | 4 | 285.1 | 286.4 | 286.8 | 287.6 | 402.0 | | | | | | 194.3 | | 686.0 | | |
| | 8 | 285.0 | 286.4 | 286.8 | 287.6 | 402.0 | | | | | | 194.3 | | 686.0 | | |
| | 12 | 285.0 | 286.4 | 286.8 | 287.5 | 402.0 | | | | | | 194.3 | | 686.0 | | |
| $[PF_6]^-$ | 2 | 285.2 | 286.6 | 287.0 | 287.7 | 402.1 | | | | | | | 136.7 | 686.8 | | |
| | 4 | 285.2 | 286.5 | 287.0 | 287.7 | 402.1 | | | | | | | 136.6 | 686.7 | | |
| | 8 | 285.0 | 286.5 | 287.0 | 287.7 | 402.1 | | | | | | | 136.6 | 686.7 | | |
| | 12 | 285.0 | 286.4 | 287.0 | 287.9 | 402.1 | | | | | | | 136.7 | 686.8 | | |
| $[TfO]^-$ | 2 | 285.3 | 286.5 | 287.0 | 287.7 | 402.0 | 292.5 | | | 532.0 | 168.4 | | | 688.5 | | |
| | 4 | 285.2 | 286.5 | 286.9 | 287.6 | 402.0 | 292.5 | | | 532.0 | 168.4 | | | 688.5 | | |
| | 8 | 285.0 | 286.4 | 286.9 | 287.6 | 402.0 | 292.5 | | | 532.0 | 168.5 | | | 688.4 | | |
| | 12 | 285.0 | 286.4 | 287.0 | 287.6 | 402.0 | 292.5 | | | 532.0 | 168.5 | | | 688.5 | | |
| $[Tf_2N]^-$ | 2 | 285.5 | 286.6 | 287.1 | 287.7 | 402.1 | 293.0 | | 399.5 | 532.7 | 169.1 | | | 688.8 | | |
| | 4 | 285.3 | 286.7 | 287.0 | 287.8 | 402.1 | 293.0 | | 399.5 | 532.7 | 169.1 | | | 688.8 | | |
| | 8 | 285.0 | 286.6 | 287.0 | 287.7 | 402.1 | 292.9 | | 399.5 | 532.7 | 169.0 | | | 688.8 | | |
| | 12 | 285.0 | 286.6 | 287.0 | 287.7 | 402.1 | 292.9 | | 399.4 | 532.7 | 169.0 | | | 688.8 | | |

[a] $N(CN^*)_2$. [b] $N^*(CN)_2$.

Fig. 9 illustrates this trend for the family of homologous liquids with the $[TfO]^-$ anion, *i.e.* $[C_nC_1Im][TfO]$. The trend was previously observed for $[C_nC_1Im][Tf_2N]$ ionic liquids,[11,21] and we now suggest that this is a general trend observed for many families of dialkylimidazolium-based ionic liquids. Consequently, unless [X] is $Cl^-$ or $Br^-$, charge correction using the $C_{aliphatic}$ 1s component in ionic liquids can only be achieved, with a high degree of confidence, when $n \geq 8$. This is confirmed by all the binding energy values of $C_{aliphatic}$ 1s in $[C_8C_1Im][X]$ and $[C_{12}C_1Im][X]$ ionic liquids being 285.0 ± 0.1 eV (Table 3).

Fig. 8 also shows that the relative shift in the binding energy of $C_{aliphatic}$ 1s with chain length is dependent upon the nature of the anion present in the liquid. The shifts following the sequence $[Tf_2N]^- > [TfO]^- \approx [N(CN)_2]^- \approx [BF_4]^- > [PF_6]^- > Cl^- \approx Br^-$. In fact $Cl^-$ and $Br^-$ showed no significant shift in the $C_{aliphatic}$ 1s binding energy at all. This sequence appears to correlate with the coordination strength of the anion, with the greatest shifts in binding energy of $C_{aliphatic}$ 1s between $n = 2$ and 8 seen in ionic liquid families with the least coordinating anions. It may be rationalised if we consider the electron density within the imidazolium ring in the presence of highly-coordinating anions. In the case of dialkylimidazolium halides, the imidazolium ring is relatively electron rich,[18,55] consequently its electron withdrawing effect on the nearby carbon atoms of the alkyl chain is minimal. If we consider the analogous system where the anion is softer in nature, *i.e.* it is larger, more delocalised and poorly coordinating, *e.g.* $[Tf_2N]^-$ and $[TfO]^-$, the imidazolium ring is relatively electron deficient and the shift in binding energy of the $C_{aliphatic}$ 1s component is more noticeable.

Clearly as the interaction between anion and cation intensifies leading to the formation of more tightly bound ion pairs, one should be able to see further spectroscopic evidence of this process occurring as electron density changes become more pronounced. Theory suggests that such anion–cation interactions are most likely to occur directly between the anion and the $C^2$ position of the imidazolium ring.[67] Spectroscopically we would expect to see shifts in the binding energies of each component of the imidazolium moiety, most significantly in the $C^2$ 1s and the $N_{cation}$ 1s. The data presented in Table 3 clearly show that the binding energies of all of the imidazolium components [$C^2$, ($C^4 + C^5$), $N_{cation}$] and ($C^6 + C^7$) are affected. This observation was also noted by Cremer *et al.*[18] However from the standpoint of charge correction, this implies that individual components drawn from the charge carrying moieties, *e.g.* the imidazolium or the anion, can only be used to charge correct samples drawn from the same family of ionic liquids bearing a common anion, *i.e.* $[C_nC_1Im][X]$, when X is common to all liquids under consideration. These components cannot be used to effect charge referencing, with any degree of confidence, across different families of

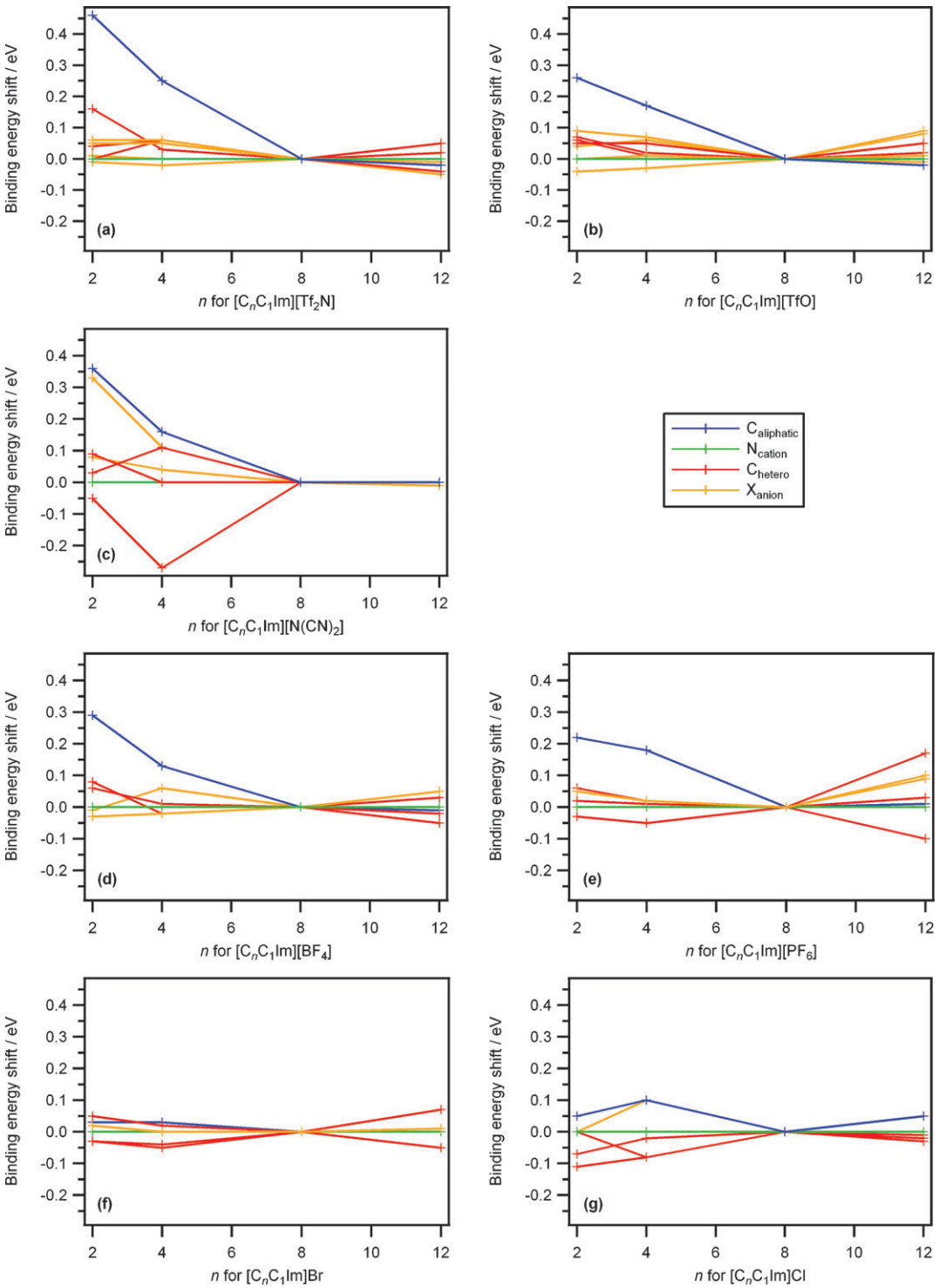


**Fig. 8** (a–g) Binding energy shifts relative to $[C_8C_1Im][X]$ as a function of alkyl chain length for each of the $[C_nC_1Im][X]$ families studied, where X = Cl, Br, $[PF_6]$, $[BF_4]$, $[Tf_2N]$, [TfO], $[N(CN)_2]$, and $n$ = 2 to 12. It should be noted that the experimental errors associated with the measurement of binding energies is of the order ±0.1 eV. The readers attention is drawn to the outliers observed in (c), this may be explained by the addition of another C 1s component when X = $[N(CN)_2]^-$. This complicates the fitting procedure for $[C_nC_1Im][N(CN)_2]$ when $n$ = 2–4; consequently we anticipate a larger degree of error in identifying the binding energies of the $C_{anion}$ 1s and ($C^4$ + $C^5$) 1s components.

ionic liquids where the nature of the anion is changing from one sample to another. For example, the measured binding energies for $N_{cation}$ 1s for $Cl^-$ and $[Tf_2N]^-$ based ionic liquids are 401.7 eV and 402.1 eV respectively. Clearly the error introduced by referencing in this way (~0.4 eV) would impact on the ability to draw conclusions from subtle changes in solute binding energies which may only be as large as 0.1 eV.

 

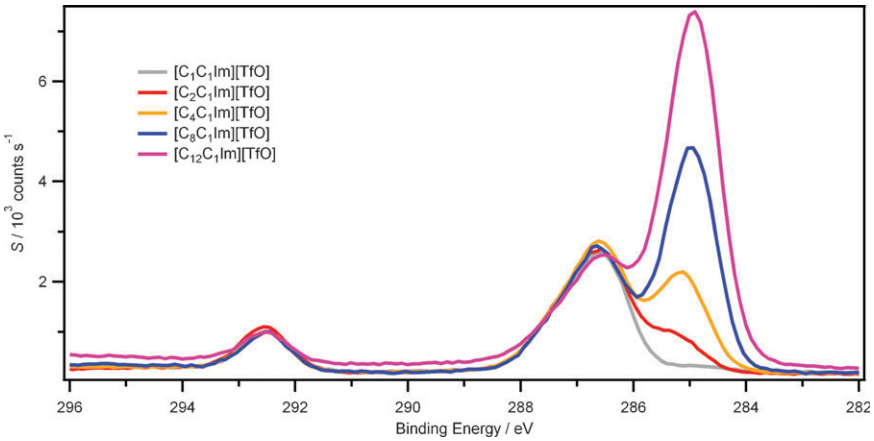


**Fig. 9** High resolution C 1s scans of different $[C_nC_1Im][TfO]$ (where $n = 1, 2, 4, 8, 12$) samples showing the shift in the binding energy peak of the $C_{aliphatic}$ 1s signal for different alkyl chains. Signal intensities are all normalised to that of the $CF_3$ peak. $[C_8C_1Im][TfO]$ was charge corrected by setting the $C_{aliphatic}$ 1s = 285.0 eV, thus a reliable binding energy for the $N_{cation}$ 1s was established; this value was then used to determine binding energies for all other members of the $[C_nC_1Im][TfO]$ family.

## Conclusions

We have demonstrated that the surfaces of ionic liquids can become positively charged when analysed by XPS, and that this is attributed to the limited electrical conductivity of the sample. Because of this surface charging and consequent shift in the measured binding energies, a charge correction method is required to provide truly comparable data sets across ionic liquid samples (both pure and those containing dissolved material). Internal referencing has been evaluated as a method for charge correcting ionic liquids using C 1s fitting models. The aliphatic carbon ($C_{aliphatic}$ 1s) moiety, present in many ionic liquids, can be used as an internal reference to charge correct XP spectra of ionic liquids containing aliphatic chains of eight carbon atoms or more. Alternatively, this method can be used to obtain the absolute binding energy of other atoms present in the anion, or indeed the binding energy of the nitrogen in the cation, $N_{cation}$ 1s. These data can then be used to charge correct ionic liquids containing the same anion and structurally similar cations that do not have a large enough aliphatic moiety to allow direct comparison using $C_{aliphatic}$ 1s methods. These methods provide charge corrected binding energies (absolute binding energies) for a wide range of commonly used imidazolium-based ionic liquids. The data tables presented in this paper may find future use as a standard list of binding energies.

## Acknowledgements

We would like to thank the EPSRC (EP/D501229/1-DICE) and the EU (SUPERGREENCHEM) for financial support. PL acknowledges the EPSRC for the award of an ARF (EP/D073014/1). The authors are grateful to Prof. H.-P. Steinrück and Dr Florian Maier for helpful discussions and critical advice.

## Notes and references

1 *Surface Analysis by Auger and X-ray Photoelectron Spectroscopy*, ed. D. Briggs and J. T. Grant, IM Publications, Chichester, 2003.
2 P. H. Citrin and T. D. Thomas, *J. Chem. Phys.*, 1972, **57**, 4446–4461.
3 M. A. Kelly, *J. Electron Spectrosc. Relat. Phenom.*, 2010, **176**, 5–7.
4 M. P. Seah, in *Surface Analysis by Auger and X-ray Photoelectron Spectroscopy*, ed. D. Briggs and J. T. Grant, IM Publications, Chichester, 2003, pp. 191–210.
5 K. Siegbahn, *Philos. Trans. R. Soc. London, Ser. A*, 1970, **268**, 33–57.
6 K. R. J. Lovelock, I. J. Villar Garcia, F. Maier, H.-P. Steinrück and P. Licence, *Chem. Rev.*, 2010, **110**, 5158–5190.
7 J. M. Gottfried, F. Maier, J. Rossa, D. Gerhard, P. S. Schulz, P. Wasserscheid and H.-P. Steinrück, *Z. Phys. Chem.*, 2006, **220**, 1439–1453.
8 H. Hashimoto, A. Ohno, K. Nakajima, M. Suzuki, H. Tsuji and K. Kimura, *Surf. Sci.*, 2010, **604**, 464–469.
9 C. Kolbeck, T. Cremer, K. R. J. Lovelock, N. Paape, P. S. Schulz, P. Wasserscheid, F. Maier and H.-P. Steinrück, *J. Phys. Chem. B*, 2009, **113**, 8682–8688.
10 C. Kolbeck, M. Killian, F. Maier, N. Paape, P. Wasserscheid and H.-P. Steinrück, *Langmuir*, 2008, **24**, 9500–9507.
11 K. R. J. Lovelock, C. Kolbeck, T. Cremer, N. Paape, P. S. Schulz, P. Wasserscheid, F. Maier and H.-P. Steinrück, *J. Phys. Chem. B*, 2009, **113**, 2854–2864.
12 K. R. J. Lovelock, E. F. Smith, A. Deyko, I. J. Villar-Garcia, P. Licence and R. G. Jones, *Chem. Commun.*, 2007, 4866–4868.
13 E. F. Smith, I. J. Villar Garcia, D. Briggs and P. Licence, *Chem. Commun.*, 2005, 5633–5635.
14 O. Höfft, S. Bahr, M. Himmerlich, S. Krischok, J. A. Schaefer and V. Kempter, *Langmuir*, 2006, **22**, 7120–7123.
15 V. Lockett, R. Sedev, C. Bassell and J. Ralston, *Phys. Chem. Chem. Phys.*, 2008, **10**, 1330–1335.
16 N. Paape, W. Wei, A. Bösmann, C. Kolbeck, F. Maier, H.-P. Steinrück, P. Wasserscheid and P. S. Schulz, *Chem. Commun.*, 2008, 3867–3869.
17 S. Caporali, U. Bardi and A. Lavacchi, *J. Electron Spectrosc. Relat. Phenom.*, 2006, **151**, 4–8.
18 T. Cremer, C. Kolbeck, K. R. J. Lovelock, N. Paape, R. Wölfel, P. S. Schulz, P. Wasserscheid, H. Weber, J. Thar, B. Kirchner, F. Maier and H.-P. Steinrück, *Chem.–Eur. J.*, 2010, **167**, 9018–9033.
19 E. F. Smith, F. J. M. Rutten, I. J. Villar-Garcia, D. Briggs and P. Licence, *Langmuir*, 2006, **22**, 9386–9392.
20 Q. H. Zhang, S. M. Liu, Z. P. Li, J. Li, Z. J. Chen, R. F. Wang, L. J. Lu and Y. Q. Deng, *Chem.–Eur. J.*, 2009, **15**, 765–778.
21 F. Maier, T. Cremer, C. Kolbeck, K. R. J. Lovelock, N. Paape, P. S. Schulz, P. Wasserscheid and H.-P. Steinrück, *Phys. Chem. Chem. Phys.*, 2010, **12**, 1905–1915.
22 H. Zhang and H. Cui, *Langmuir*, 2009, **25**, 2604–2612.
23 J. P. Mikkola, P. Virtanen, H. Karhu, T. Salmi and D. Y. Murzin, *Green Chem.*, 2006, **8**, 197–205.
24 F. Neaţu, V. I. Pârvulescu, V. Michelet, J. P. Gênet, A. Goguet and C. Hardacre, *New J. Chem.*, 2009, **33**, 102–106.

25 M. D. Nguyen, L. V. Nguyen, E. H. Jeon, J. H. Kim, M. Cheong, H. S. Kim and J. S. Lee, *J. Catal*., 2008, **258**, 5–13.
26 D. S. Silvester, T. L. Broder, L. Aldous, C. Hardacre, A. Crossley and R. G. Compton, *Analyst*, 2007, **132**, 196–198.
27 R. T. Tao, S. D. Miao, Z. M. Liu, Y. Xie, B. X. Han, G. M. An and K. L. Ding, *Green Chem*., 2009, **11**, 96–101.
28 F. L. Qiu, A. W. Taylor, S. Men, I. J. Villar-Garcia and P. Licence, *Phys. Chem. Chem. Phys*., 2010, **12**, 1982–1990.
29 A. W. Taylor, F. L. Qiu, I. J. Villar-Garcia and P. Licence, *Chem. Commun*., 2009, 5817–5819.
30 J. F. Moulder, W. F. Stickle, P. E. Sobol and K. D. Bomben, *Handbook of X-ray photoelectron spectroscopy: a reference book of standard spectra for identification and interpretation of XPS data*, Physical Electronics, Eden Prairie, MN, 1995.
31 M. A. Kelly, in *Surface Analysis by Auger and X-ray Photoelectron Spectroscopy*, ed. D. Briggs and J. T. Grant, IM Publications, Chichester, 2003, pp. 191–210.
32 *High Resolution XPS of Organic Polymers: The Scienta ESCA300 Database*, ed. G. Beamson and D. Briggs, John Wiley and Sons, Chichester, 1992; Also available as a CD-ROM, *The XPS of Polymers Database*, ed. G. Beamson and D. Briggs, Surface Spectra, Manchester, 2000.
33 R. T. Lewis and M. A. Kelly, *J. Electron Spectrosc. Relat. Phenom*., 1980, **20**, 105–115.
34 *British Standards*, 2004, BS ISO 19318:12004.
35 A. Cros, *J. Electron Spectrosc. Relat. Phenom*., 1992, **59**, 1–14.
36 S. Krischok, M. Eremtchenko, M. Himmerlich, P. Lorenz, J. Uhlig, A. Neumann, R. Öttking, W. J. D. Beenken, O. Höfft, S. Bahr, V. Kempter and J. A. Schaefer, *J. Phys. Chem. B*, 2007, **111**, 4801–4806.
37 F. Bernardi, J. D. Scholten, G. H. Fecher, J. Dupont and J. Morais, *Chem. Phys. Lett*., 2009, **479**, 113–116.
38 R. Fortunato, C. A. M. Afonso, J. Benavente, E. Rodríguez-Castellón and J. G. Crespo, *J. Membr. Sci*., 2005, **256**, 216–223.
39 H. Kamimura, T. Kubo, I. Minami and S. Mori, *Tribol. Int*., 2007, **40**, 620–625.
40 J. H. Kwon, S. W. Youn and Y. C. Kang, *Bull. Korean Chem. Soc*., 2006, **27**, 1851–1853.
41 W. M. Liu, C. F. Ye, Q. Y. Gong, H. Z. Wang and P. Wang, *Tribol. Lett*., 2002, **13**, 81–85.
42 Q. M. Lu, H. Z. Wang, C. F. Ye, W. M. Liu and Q. J. Xue, *Tribol. Int*., 2004, **37**, 547–552.
43 J. P. T. Mikkola, P. P. Virtanen, K. Kordas, H. Karhu and T. O. Salmi, *Appl. Catal., A*, 2007, **328**, 68–76.
44 C. Paun, C. Stere, S. M. Coman, V. I. Pârvulescu, P. Goodrich and C. Hardacre, *Catal. Today*, 2008, **131**, 98–103.
45 K. Kanai, T. Nishi, T. Iwahashi, Y. Ouchi, K. Seki, Y. Harada and S. Shin, *J. Chem. Phys*., 2008, **129**, 224507.
46 M. Shigeyasu, H. Murayama and H. Tanaka, *Chem. Phys. Lett*., 2008, **463**, 373–377.
47 J. S. Wilkes, J. A. Levisky, R. A. Wilson and C. L. Hussey, *Inorg. Chem*., 1982, **21**, 1263–1264.
48 J. G. Huddleston, A. E. Visser, W. M. Reichert, H. D. Willauer, G. A. Broker and R. D. Rogers, *Green Chem*., 2001, **3**, 156–164.
49 P. Bonhôte, A.-P. Dias, M. Armand, N. Papageorgiou, K. Kalyanasundaram and M. Grätzel, *Inorg. Chem*., 1998, **37**, 166–166.
50 P. Bonhôte, A.-P. Dias, N. Papageorgiou, K. Kalyanasundaram and M. Grätzel, *Inorg. Chem*., 1996, **35**, 1168–1178.
51 P. A. Z. Suarez, J. E. L. Dullius, S. Einloft, R. F. De Souza and J. Dupont, *Polyhedron*, 1996, **15**, 1217–1219.
52 H. Tokuda, K. Hayamizu, K. Ishii, M. A. B. H. Susan and M. Watanabe, *J. Phys. Chem. B*, 2004, **108**, 16593–16600.
53 C. Jork, C. Kristen, D. Pieraccini, A. Stark, C. Chiappe, Y. A. Beste and W. Arlt, *J. Chem. Thermodyn*., 2005, **37**, 537–558.
54 J. D. Holbrey, W. M. Reichert, R. P. Swatloski, G. A. Broker, W. R. Pitner, K. R. Seddon and R. D. Rogers, *Green Chem*., 2002, **4**, 407–413.
55 I. J. Villar-Garcia, *PhD Thesis*, University of Nottingham, 2009.
56 The derivation of the Kratos sensitivity factors is not documented, although it is believed that they have been adapted from early values published by C. D. Wagner, *et al*., *Surf. Interface Anal*., 1981, **3**, 211–225.
57 N. Fairley and A. Carrick, *The Casa Cookbook*, Acolyte Science, Knutsford, UK, 2005.
58 G. Beamson, D. T. Clark, J. Kendrick and D. Briggs, *J. Electron Spectrosc. Relat. Phenom*., 1991, **57**, 79–90.
59 D. Briggs and G. Beamson, *Anal. Chem*., 1992, **64**, 1729–1736.
60 S. Ardizzone, C. L. Bianchi, M. Fadoni and B. Vercelli, *Appl. Surf. Sci*., 1997, **119**, 253–259.
61 R. Dedryvère, S. Leroy, H. Martinez, F. Blanchard, D. Lemordant and D. Gonbeau, *J. Phys. Chem. B*, 2006, **110**, 12986–12992.
62 U. Gelius, P. F. Hedén, J. Hedman, B. J. Lindberg, R. Manne, R. Nordberg, C. Nordling and K. Siegbahn, *Phys. Scr*., 1970, **2**, 70–80.
63 B. J. Lindberg and J. Hedman, *Chem. Scr*., 1975, **7**, 155–166.
64 R. Nordberg, R. G. Albridge, T. Bergmark, U. Ericson, J. Hedman, C. Nordling, K. Siegbahn and B. J. Lindberg, *Ark. Kemi*, 1968, **28**, 257.
65 C. D. Wagner, L. H. Gale and R. H. Raymond, *Anal. Chem*., 1979, **51**, 466–482.
66 J. N. Canongia Lopes and A. A. H. Pádua, *J. Phys. Chem. B*, 2006, **110**, 3330–3335.
67 P. A. Hunt, B. Kirchner and T. Welton, *Chem.–Eur. J*., 2006, **12**, 6762–6775.


 